Journal of Hazardous Materials 183 (2010) 271–278

Contents lists available at ScienceDirect

Journal of Hazardous Materials

journal homepage: www.elsevier.com/locate/jhazmat

Catalytic ozonation of fenofibric acid over alumina-supported manganese oxide

Roberto Rosal*, María S. Gonzalo, Antonio Rodríguez, Eloy García-Calvo

Departamento de Química Analítica e Ingeniería Química, Universidad de Alcalá, E-28771 Alcalá de Henares, Spain

ARTICLE INFO

Article history:
Received 4 May 2010
Received in revised form 1 July 2010
Accepted 6 July 2010
Available online 13 July 2010

Keywords:
Heterogeneous catalytic ozonation
Manganese oxide
Fenofibric acid
Adsorption
Hydroxyl radicals

ABSTRACT

The catalytic ozonation of fenofibric acid was studied using activated alumina and alumina-supported manganese oxide in a semicontinuous reactor. The rate constants at 20 °C for the non-catalytic reaction of fenofibric acid with ozone and hydroxyl radicals were $3.43 \pm 0.20\ M^{-1}\ s^{-1}$ and $(6.55 \pm 0.33) \times 10^9\ M^{-1}\ s^{-1}$, respectively. The kinetic constant for the catalytic reaction between fenofibric acid and hydroxyl radicals did not differ significantly from that of homogeneous ozonation, either using Al_2O_3 or MnO_x/Al_2O_3. The results showed a considerable increase in the generation of hydroxyl radicals due to the use of catalysts even in the case of catalytic runs performed using a real wastewater matrix. Both catalysts promoted the decomposition of ozone in homogeneous phase, but the higher production of hydroxyl radicals corresponded to the catalyst with more activity in terms of ozone decomposition. We did not find evidence of the catalysts having any effect on rate constants, which suggests that the reaction may not involve the adsorption of organics on catalyst surface.

1. Introduction

Fenofibrate is a drug prescribed worldwide to reduce plasma triglycerides, which is metabolized through the hydrolytic cleavage of carboxyl ester moiety resulting in 2-[4-(4-chlorobenzoyl)phenoxy]-2-methylpropanoic acid, usually referred to as fenofibric acid. The presence of fenofibric acid has been repeatedly reported. Stump et al. found concentrations of up to $500\ ng\ L^{-1}$ in the influent of several Brazilian WWTP [1]. In Europe, Ternes et al. reported $130\ ng\ L^{-1}$ of fenofibric acid in the effluent of a German WWTP [2]. Acero et al. found $180\ ng\ L^{-1}$ in a secondary effluent from a municipal WWTP located in Móstoles, Madrid, Spain [3]. Rodríguez et al. [4] and Rosal et al. [5] reported $165\ ng\ L^{-1}$ and $129\ ng\ L^{-1}$ respectively of fenofibric acid in the effluent of a WWTP located in Madrid.

The high toxicity of fenofibric acid for several aquatic microorganisms has recently been assessed [6]. The release of complex mixtures of such biologically active chemicals severely jeopardises the reuse of treated wastewater, a reasonable solution to achieve a sustainable water cycle management [7]. The removal of organic compounds in wastewater can be performed by means of advanced oxidation processes that are those in which hydroxyl radicals represent the primary oxidant species [8]. Among them, heterogeneous catalytic ozonation has received attention due to the simplicity of catalyst recovery. It is also a choice to limit the formation of oxidation intermediates [9,10]. Alumina and alumina-supported metal oxides exhibit a high activity for the gas phase ozone-assisted oxidation of volatile pollutants [11]. In aqueous phase, Yang et al. [12] showed that the removal of dissolved organics is significantly enhanced by the presence of mesoporous alumina-supported manganese oxide. The mechanism for heterogeneous catalytic ozonation involve the adsorption of ozone or its decomposition at specific sites on the surface. The main discrepancy between models consists in whether or not the chemisorption of the organic compound takes place. The adsorption of dissolved neutral compounds on metal oxides is limited due to the competitive adsorption of water molecules, but ionizable organics may adsorb if the surface is charged and allows ion exchange. This is the case of metal oxides, which behave as anion (cation) exchangers if the pH of the solution is below (above) the point of zero charge of the surface [13]. Although it is generally true that the extent of adsorption considerably decreases under the unfavourable electrostatic conditions that take place on charged surfaces, it has been pointed out that small but significant adsorption may occur even in this case through surface complexation reactions [14].

The objective of the present study was to use kinetic data to highlight the mechanism by which solid catalysts enhance the rate of ozonation in aqueous solution and to determine whether or not the possible adsorption of organics on catalytic surfaces results in a change of rate constants. To this end, we performed kinetic experiments either in pure water and wastewater and studied the extent to which the catalysts

* Corresponding author. Tel.: +34 918855099; fax: +34 918855088.
E-mail address: roberto.rosal@uah.es (R. Rosal).

0304-3894/$ – see front matter © 2010 Elsevier B.V. All rights reserved.
doi:10.1016/j.jhazmat.2010.07.021

Nomenclature

r_{FFA}	fenofibric acid oxidation rate in homogeneous units (mol L^{-1} s^{-1})
k_{O_3}	second order rate constant for direct ozonation reaction (L mol^{-1} s^{-1})
$k_{HO\bullet}$	second order rate constant for the reaction with hydroxyl radicals (L mol^{-1} s^{-1})
c_A	concentration of a given organic compound (mol L^{-1})
$c_{HO\bullet}$	concentration of hydroxyl radical (mol L^{-1})
c_{O_3}	concentration of dissolved ozone (mol L^{-1})
$c^*_{O_3}$	equilibrium concentration of dissolved ozone (mol L^{-1})
Ha	Hatta number
ν	stoichiometric coefficient
k_R	second order apparent homogeneous rate constant (L mol^{-1} s^{-1})
D_{O_3}	ozone diffusivity (m^2 s^{-1})
k_L	liquid phase individual mass transfer coefficient (m s^{-1})
k_La	volumetric mass transfer (s^{-1})
R_{ct}	ratio of $c_{HO\bullet}$ to c_{O_3}
$\bar{R}_{ct}$	average value of R_{ct} defined in Eq. (8)
m	parameter defined in Eq. (5)

Subscripts and superscripts

FFA	fenofibric acid
ATZ	atrazine
0	initial
t	generic reaction time
*	equilibrium
h	homogeneous reaction
c	catalytic reaction
hc	simultaneous homogeneous and catalytic reaction

increased the concentration of hydroxyl radicals derived from ozone.

2. Experimental

2.1. Materials

Atrazine and *tert*-butyl alcohol (*t*-BuOH) supplied by Sigma–Aldrich were high-purity analytical grade reagents. Fenofibric acid was produced as indicated elsewhere [6]. MiliQ ultrapure water with a resistivity of at least 18 MΩ cm at 25 °C was obtained from a Milipore system. The catalysts used in this study were alumina (γ-Al_2O_3) and alumina-supported manganese oxide (MnO_x/Al_2O_3). γ-Al_2O_3 was purchased from Sigma–Aldrich and used as received. Its surface area was 155 m^2 g^{-1}, determined by nitrogen adsorption, and its average particle size was 100 μm. The MnO_x/Al_2O_3 catalyst was prepared by incipient wetness impregnation dried γ-Al_2O_3 using an aqueous solution of $Mn(CH_3COO)_2{\cdot}4H_2O$ (Sigma–Aldrich). The catalyst was subsequently dried in air at 423 K and calcined at 773 K for 3 h. The catalyst was washed twice in PBW to avoid further leaching of manganese. The amount of manganese used corresponded to a 10 wt% of MnO_2. The BET surface area was 119 m^2 g^{-1}. The isoelectric point (IEP) of the catalysts was obtained by measuring the ζ-potential in aqueous solutions at 25 °C after adjusting ionic strength to 10^{-3} M with NaCl. The values obtained for IEP were 8.2 for γ-Al_2O_3 and 7.3 for MnO_x/Al_2O_3 as prepared, which fell to 3.0 for MnO_x/Al_2O_3 after contact with bubbling ozone in aqueous slurry for 30 min.

Table 1
Main wastewater parameters.

pH	8.2
Total suspended solids (mg L^{-1})	13
Conductivity (μS cm^{-1})	624
COD (mg L^{-1})	83
TOC (mg L^{-1})	14.3
PO_4-P (mg L^{-1})	0.15
Anions and cations (mg L^{-1})	
Fluoride	0.1
Chloride	133.1
Nitrite	0.3
Nitrate	8.2
Sulfate	67.2
Carbonate	2.8
Bicarbonate	114.8
Sodium	116.4
Potassium	19.2
Ammonium	11.9
Magnesium	7.1
Calcium	27.4

Wastewater was collected from the secondary clarifier of a WWTP located in Colmenar Viejo (Madrid). The plant operates with a conventional activated sludge treatment, has a capacity of 53 000 equivalent inhabitants and was designed to treat a maximum volume of wastewater of 8000 m^3 day^{-1}. The main characteristics of treated wastewater are shown in Table 1.

2.2. Ozonation procedure

The ozonation runs were performed in a 1 L glass jacketed reactor whose temperature was controlled at 20 °C using a thermostatic regulator. For experiments with spiked wastewater and non-buffered pure water, pH was controlled at 6.5 within ±0.1 units by means of a feed-back control device that delivered a solution of sodium hydroxide though a LC10AS Shimadzu pump. The rest of the runs were performed in solutions adjusted to pH 6.5 using a 0.1 M phosphate buffered water (PBW). Ozone was produced by a corona discharge and continuously bubbled throughout the run with a gas flow of 0.20 N m^3 h^{-1}. Further details are given elsewhere [15].

The experiments using fenofibric acid in pure water were conducted with a concentration of fenofibric acid in the 5–15 mg L^{-1} range (16–47 mM) and, in certain runs, *t*-BuOH at 5 mg L^{-1} (67 μM), 74 mg L^{-1} (1.0 mM) and 741 mg L^{-1} (10 mM), in order to inhibit or suppress the contribution of the radical reaction. Atrazine was added at a concentration of up to 2 mg L^{-1} as reference compound [16]. In the samples withdrawn for analysis, dissolved ozone was removed either by the addition of sodium thiosulfate or by bubbling nitrogen at a flow-rate of about 0.2 N m^3 h^{-1}. For the later, we could check that the concentration of ozone fell below 3% in less than 30 s.

For the experiments with spiked wastewater, the prescribed amount of fenofibric acid was dissolved in raw wastewater whose pH was previously adjusted to 6.5 with HCl. In these runs fenofibric acid and atrazine were dissolved in wastewater previously ozonated until ozone appeared in solution. The reason for this procedure was to avoid interferences due to the presence of organic compounds that react rapidly with ozone [17].

In all catalytic runs, the catalyst was pre-oxidized prior to the addition of organics for 15 min with the same ozone flow as that used for ozonation runs. In samples taken from catalytic runs, pH was raised to >8.5 with NaOH and stirred continuously for at least 30 min prior to filtering using 0.22 μm Millex-GV PVDF Millipore filters. The aim of this procedure was to avoid the loss of organics adsorbed on the catalyst surface by displacing them with a

strong base. Certain ozone decomposition experiments were also performed by stopping the gas flow at a given moment using a procedure described elsewhere [18].

2.3. Analyses

The concentration of ozone dissolved in the aqueous phase was monitored with an amperometric Rosemount 499AOZ analyzer periodically calibrated using the Indigo Colorimetric Method (SM 4500-O3 B). A data acquisition unit digitalized the signals from the concentration of dissolved ozone, pH and temperature with a sampling period of 1 s. The concentration of ozone in gas phase was determined using an Anseros Ozomat GM6000 Pro photometer calibrated against potassium iodide. Total Organic Carbon (TOC) was determined by means of a Shimadzu TOC-VCSH total carbon organic analyzer equipped with an ASI-V autosampler. The BET specific surface was determined by nitrogen adsorption at 77 K using a SA 3100 Beckman Coulter Analyzer. Anions were determined using a Metrohm 861 Advance Compact IC with suppressed conductivity detector and a Metrosep A Supp 7-250 analytical column with 36 mM Na_2CO_3 as eluent with a flow of 0.8 mL min^{-1}. Cations were quantified by means of a Metrosep C3 column using 5.0 mM HNO_3 as eluent with a flow of 1 mL min^{-1}. The analyses of fenofibric acid and atrazine were performed by HPLC using a Hewlett Packard 1200 Series apparatus (Agilent Technologies, Palo Alto, USA) equipped with a reversed phase Kromasil 5u 100A C18 analytical column. UV detection was carried out at 280 nm (fenofibric acid) and 228 nm (atrazine). To allow statistical analysis to be performed, runs were replicated and all HPLC determinations were carried out in quintuplicate.

3. Results and discussion

The kinetics of a gas–liquid ozonation process depends on the relative rates of physical absorption and chemical reaction. The kinetic regime is determined by the Hatta number, which represents the maximum rate of chemical reaction relative to the maximum rate of mass transfer. For a second order reaction, the Hatta number is:

$$Ha = \frac{\sqrt{\nu k_R c_A D_{O_3}}}{k_L} \quad (1)$$

in which k_R is the second order homogeneous rate constant based on the depletion of the organic compound, D_{O_3} the diffusivity of ozone in water (1.77×10^{-9} m^2 s^{-1}) and c_A the concentration of substance to be oxidized. An estimation of the mass transfer coefficient, $k_L = 5.5 \times 10^{-5}$ m s^{-1}, was obtained according to Calderbank and Moo-Young [19]. Using initial concentrations, c_{A0} as those corresponding to the most unfavourable conditions, we found that all results reported in what follows corresponded to slow kinetic regime ($Ha < 0.4$). This was confirmed by a criterion based on appearance of ozone in solution that was explained in a previous work [5]. The upper boundary for the stoichiometric coefficient was estimated by relating the moles of ozone transferred to the liquid phase to the amount of fenofibric acid oxidized at a given time:

$$\nu < \frac{k_L a c^*_{O_3} t - k_L a \int_0^t c_{O_3}\, dt}{c_A - c_{A0}} \quad (2)$$

The volumetric mass transfer coefficient, $k_L a$, was determined in transient runs with pure water and $c^*_{O_3}$ is the equilibrium concentration of ozone in the liquid calculated from Henry's law. Details are given elsewhere [20]. This procedure yielded a value of $\nu \sim 2$. In addition to catalytic ozonation runs, the adsorption of fenofibric acid on the catalyst surface was assessed. Fenofibric acid, whose pK_a is 2.9, dissociates in aqueous solution even under acidic conditions. The adsorption of dissociated acids is favoured when the surface can behave as an anion exchanger, but is hindered by the presence of dissolved salts. After 24 h in contact with Al_2O_3 and MnO_x/Al_2O_3, the amount adsorbed was near 10% (initial concentration 15 mg L^{-1}, amount of catalyst 1 g L^{-1}) in pure water but fell below statistical significance in PBW and wastewater. Particularly, the amount adsorbed was not significantly different from zero in any case after one hour. Other studies have reported the lack of adsorption of organics on various catalysts including supported manganese oxide at several pH values [10]. It should be noted that the isoelectric point of manganese oxides is strongly dependent on its oxidation state and crystallographic form. Manganese oxide-supported catalysts exist as multivalent oxidation states that under heat treatments proceed from MnO_2, to Mn_2O_3 and Mn_3O_4 [21]. Mn_2O_3 is the form with the highest IEP, in the 7.6–9.0 range, which probably dominates the MnO_x/Al_2O_3 catalyst prior to contact with ozone [22]. The fact that IEP in aqueous slurry in the presence of ozone fell to 3.0, a value typical for tetrahedrally coordinated Mn^{4+}, is consistent with the assumption that MnO_2 was the main species in manganese oxide catalysts in contact with ozone. The oxidation of MnO_x/Al_2O_3 catalysts by ozone to their higher oxidation state has been observed in gas phase [23].

3.1. Non-catalytic ozonation

Fenofibric acid's depletion rate is the consequence of its second order parallel reaction with dissolved ozone and with hydroxyl radicals:

$$r^h_{FFA} = k^h_{O_3} c_{FFA} c_{O_3} + k^h_{HO\bullet} c_{FFA} c_{HO\bullet} \quad (3)$$

According to the hypothesis proposed by Elovitz and von Gunten, the ozonation process is characterized by a parameter defined as the relationship between the ratio of the concentration of hydroxyl radicals and ozone that represents the efficiency of the system in generating hydroxyl radicals [24].

$$r^h_{FFA} = (k^h_{O_3} + k^h_{HO\bullet} R^h_{ct}) c_{FFA} c_{O_3} \quad (4)$$

A mass balance to fenofibric acid in the reactor leads to a differential equation, $r^h_{FFA} = -dc_{FFA}/dt$, that can be readily integrated if R^h_{ct}, the ratio of $c_{HO\bullet}$ to c_{O_3} in homogeneous conditions, is constant throughout the run:

$$\ln\left(\frac{c_{FFA(0)}}{c_{FFA(t)}}\right) = (k^h_{O_3} + k^h_{HO\bullet} R^h_{ct}) \int_0^t c_{O_3}\ dt = k^h_R \int_0^t c_{O_3} dt \quad (5)$$

This situation has been encountered in a previous work with a real non-spiked wastewater matrix [5]. If this is not the case and R_{ct} is variable, the corresponding mass balance has to be written in discrete form as indicated below. The data represented in Fig. 1, corresponding to runs performed in PBW in the presence of *t*-BuOH 10 mM as hydroxyl radical scavenger, allowed $k^h_{O_3}$ to be calculated for fenofibric acid, yielding 3.43 ± 0.20 M^{-1} s^{-1}, a relatively low constant for the direct ozonation reaction. The linear relationship of the logarithmic concentration decay with integral ozone exposure indicates a constant value for R^h_{ct}. In the same figure, we represented the data for atrazine, also in 10 mM *t*-BuOH, with a direct ozonation constant of 7.43 ± 0.11 M^{-1} s^{-1}, a result in good agreement with the value previously given by von Gunten [25]. As usual, boundaries represent 95% confidence intervals. The well-known competition method was used with atrazine as reference compound. Assuming a constant hydroxyl radical-to-ozone ratio, the following expression can be derived:

$$\ln\left(\frac{c_{FFA\ (0)}}{c_{FFA\ (t)}}\right) = \frac{k^h_{O_3\,(FFA)} + k^h_{HO\bullet\,(FFA)} R^h_{ct}}{k^h_{O_3\,(ATZ)} + k^h_{HO\bullet\,(ATZ)} R^h_{ct}} \ln\left(\frac{c_{ATZ(0)}}{c_{ATZ(t)}}\right) = m\ \ln\left(\frac{c_{ATZ(0)}}{c_{ATZ(t)}}\right) \quad (6)$$

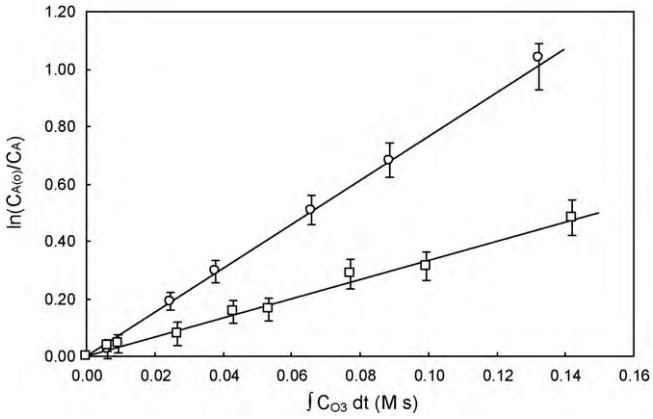

Fig. 1. Logarithmic decay of the concentration of fenofibric acid (□) and atrazine (○) in non-catalytic ozonation runs carried out with *t*-BuOH 10 mM as a function of integral ozone exposure (pH 6.5).

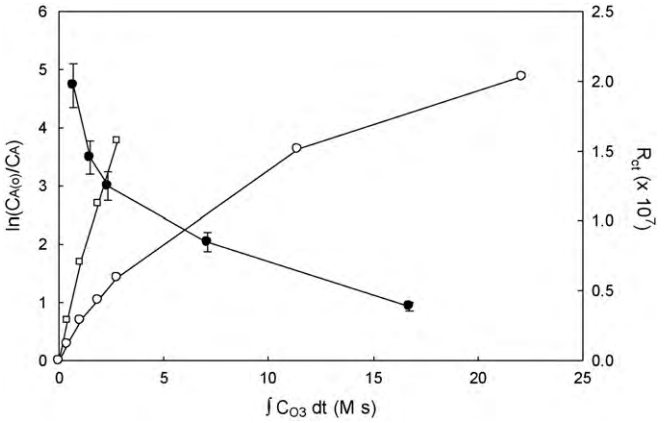

Fig. 3. Concentration of fenofibric acid (□) and atrazine (○) during a non-catalytic ozonation process as a function of the integral ozone exposure (pH 6.5). The secondary axis and filled circles represent the average R_{ct} values.

As the direct ozonation rate constants for fenofibric acid and atrazine are low, a plot of $\ln(c_{FFA(0)}/c_{FFA})$ versus $\ln(c_{ATZ(0)}/c_{ATZ})$ would yield a straight line with a slope $m = k^{h}_{HO^{\bullet}(FFA)}/k^{h}_{HO^{\bullet}(ATZ)}$; this also holds true for non-constant R^{h}_{ct} [26]. The values reported in the literature for the reaction of atrazine with hydroxyl radical are $3 \times 10^9\ M^{-1}\ s^{-1}$ [27], $(2.54 \pm 0.22) \times 10^9\ M^{-1}\ s^{-1}$ [28] and $2.4 \times 10^9\ M^{-1}\ s^{-1}$ [29]. Fig. 2 shows the experimental relationship the concentration decays of fenofibric acid and atrazine for runs performed in PBW. The value obtained in this study for $k^{h}_{HO^{\bullet}(FFA)}$ was $(6.55 \pm 0.33) \times 10^9\ M^{-1}\ s^{-1}$, which used the value of Balci et al. for $k^{h}_{HO^{\bullet}(ATZ)}$, the only indicating uncertainty [28]. The boundaries represent 95% confidence intervals and take into account the experimental error for $k^{h}_{HO^{\bullet}(ATZ)}$ indicated by Balci et al. [28]. Fig. 3 shows the conversion of fenofibric acid and atrazine as a function of integral ozone exposure. The data, particularly those for atrazine, indicate that k^{h}_{R} changed in the course of the run. In this case, instead of Eq. (5), a discrete form can be written for short time intervals as follows:

$$\ln\left(\frac{c_{ATZ(t)}}{c_{ATZ(t+\Delta t)}}\right) = (k^{h}_{O_3(ATZ)} + k^{h}_{HO^{\bullet}(ATZ)}\bar{R}^{h}_{ct}) \int_{t}^{t+\Delta t} c_{O_3}\ dt \qquad (7)$$

The value $\bar{R}^{h}_{ct}$ represents the average hydroxyl radical-to-ozone ratio within the interval $(t, t+\Delta t)$ defined as follows:

$$\bar{R}^{h}_{ct} = \frac{\int_{t}^{t+\Delta t} R_{ct} c_{O_3}\ dt}{\int_{t}^{t+\Delta t} c_{O_3}\ dt} \qquad (8)$$

The experimental set-up allowed accurate and continuous determination of the concentration of dissolved ozone and, therefore, of integral ozone exposure. The results for $\bar{R}^{h}_{ct}$ for the non-catalytic ozonation of fenofibric acid in PBW are also shown in Fig. 3 and range from 2×10^{-7} at the beginning of the run to 4.7×10^{-8} for an integral ozone exposure of 16.5 mM s.

In the experiments performed using wastewater, the reaction mixture was not loaded with phosphate buffer, the pH being controlled by the closed-loop control device described above. The wastewater was spiked with fenofibric and atrazine at the same initial concentrations indicated before. In this case, the logarithmic concentration decays of fenofibric acid and atrazine were linear, as shown in Fig. 4. The value of R^{h}_{ct} obtained from Eq. (6) was 9.4×10^{-10}, considerably lower than that obtained for pure water or PBW, but within the broad range of usual R_{ct} values, which typically fall in the 10^{-6} to 10^{-10} range [30].

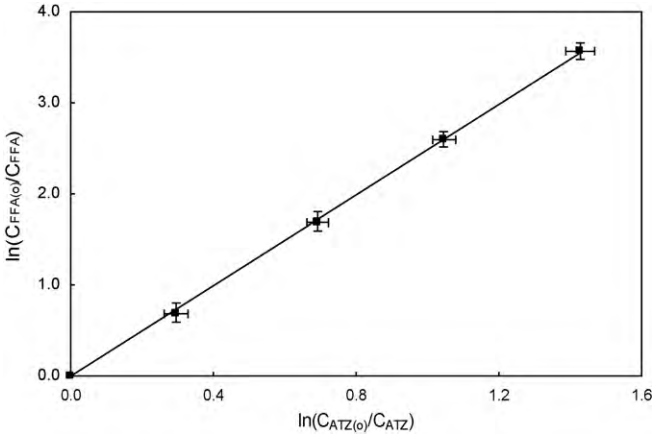

Fig. 2. Logarithmic plot of the concentration of fenofibric acid and atrazine in non-catalytic ozonation runs (pH 6.5).

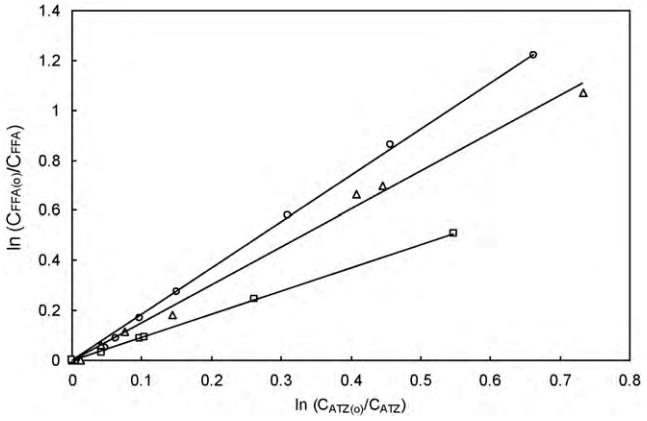

Fig. 4. Logarithmic plot of the concentration of fenofibric acid and atrazine in non-catalytic ozonation (□) and using 1 g L^{-1} Al_2O_3 (△) and 1 g L^{-1} MnO_x/Al_2O_3 (○) for initial concentration of fenofibric acid of 15 mg L^{-1} in wastewater. (pH 6.5; error bars not shown for clarity.)

3.2. Catalytic ozonation

In catalytic ozonation, the reaction may take place between organic compounds and hydroxyl radicals with at least one of them being adsorbed. Assuming adsorption equilibrium and low surface coverage, the rate expression becomes linear with the concentration of adsorbate:

$$r^{c}_{FFA} = k^{c}_{O_3} c_{FFA} c_{O_3} + (k^{h}_{HO\bullet} R^{h}_{ct} c_{FFA} c_{O_3} + k^{c}_{HO\bullet} R^{c}_{ct} c_{FFA} c_{O_3}) \quad (9)$$

Details concerning the derivation of the former equation are given elsewhere [4,18]. As stated above, fenofibric acid, even dissociated at the working pH, adsorbed to a very low degree. In addition, the catalysts has no significant effect on the direct ozonation constant in the presence of *t*-BuOH. Consequently, we assumed that the direct ozonation of fenofibric acid was a non-catalytic process and $k^{c}_{O_3\,(FFA)} = k^{h}_{O_3\,(FFA)}$.

Indirect ozonation is usually considered to be the combination of a homogeneous and a catalytic process. In this work we used atrazine to derive the hydroxyl radical-to-ozone ratio as indicated in Eq. (7). Atrazine is a neutral compound for which the amount adsorbed on both catalysts was not statistically significant whether in pure water, PBW or wastewater. Therefore, the experimental ratio R_{ct} was measured in the bulk in both catalytic and non-catalytic runs. As a consequence, R^{h}_{ct} and R^{c}_{ct} correspond to the same property and have been represented in what follows by the same symbol, R^{hc}_{ct}:

$$r^{c}_{FFA} = k^{c}_{O_3} c_{FFA} c_{O_3} + (k^{h}_{HO\bullet} + k^{c}_{HO\bullet}) R^{hc}_{ct} c_{FFA} c_{O_3} \quad (10)$$

Taking $k^{hc}_{HO\bullet}$ to denote the apparent kinetic constant for the reaction with hydroxyl radicals in the presence of catalyst, the kinetic equation yields the same mathematical form obtained before for homogeneous ozonation:

$$r^{c}_{FFA} = k^{h}_{O_3} c_{FFA} c_{O_3} + k^{hc}_{HO\bullet} R^{hc}_{ct} c_{FFA} c_{O_3} \quad (11)$$

The adsorption of reactive species should be reflected in significant differences between $k^{hc}_{HO\bullet}$ and $k^{h}_{HO\bullet}$, which can be checked by means of kinetic data. Combined with the mass balance and on integration, Eq. (11) leads to expressions formally identical to those derived for non-catalytic runs. The results corresponding to the catalytic ozonation of fenofibric acid in spiked wastewater using Al_2O_3 and MnO_x/Al_2O_3 are shown in Fig. 4. This plot, representing the competition kinetic method, was linear for both catalysts, but the change in slope for different catalysts and for catalytic runs with respect to non-catalytic ozonation does not necessarily mean that $k^{hc}_{HO\bullet}$ and $k^{h}_{HO\bullet}$ were different. This is shown in Fig. 5, where we plotted the slope *m* of Eq. (6) as a function of hydroxyl radical-to-ozone ratio, R_{ct}. The solid line corresponds to $k^{h}_{HO\bullet\,(FFA)} = 6.55 \times 10^{9}\ M^{-1}\ s^{-1}$, measured for non-catalytic conditions, so that the results from non-catalytic runs are expected to be distributed along it. The dashed line represents an arbitrary

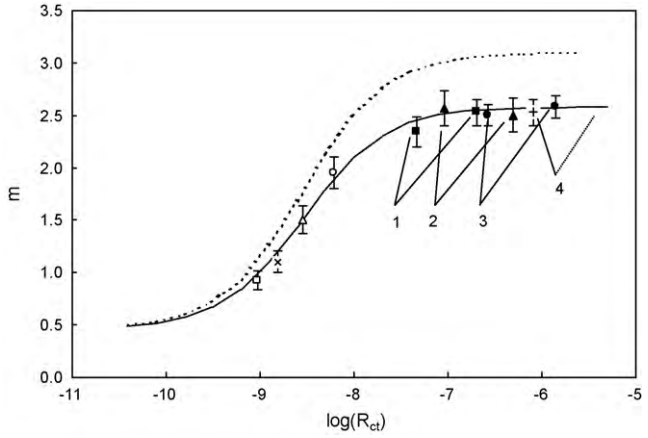

Fig. 5. Parameter *m* defined in Eq. 6 as a function of R_{ct} for non-catalytic runs (□) and experiments using Al_2O_3 (△) and MnO_x/Al_2O_3 (○) in wastewater. Filled symbols represent the same runs in PBW: non-catalytic (1, ■), Al_2O_3 (2, ▲) and MnO_x/Al_2O_3 (3, ●). For these and also for MnO_x/Al_2O_3 (4, +) in pure – not buffered – water (4, +), the span represents the change in R_{ct} from the first minute to the average between 5 min and 8 min. The cross (×) corresponds to ozonation PBW + 1.0 mM *t*-BuOH using MnO_x/Al_2O_3. pH was 6.5 in all cases.

20% increase in $k^{h}_{HO\bullet\,(FFA)}$ with respect to the non-catalytic reaction. If the catalytic reaction with hydroxyl radicals involved adsorbed organics, it might be expected that the rate constant $k^{hc}_{HO\bullet}$ would differ from that of the homogeneous system, $k^{h}_{HO\bullet}$. By combining the results of $\bar{R}^{hc}_{ct}$ (Eq. (7)) with *m* (Eq. (6)), the points corresponding to catalytic and non-catalytic reactions can be located in Fig. 5. The results from catalytic ozonation in the wastewater matrix, represented as empty symbols, show that there was no significant difference between $k^{hc}_{HO\bullet}$ and the homogeneous ratio $k^{h}_{HO\bullet}$.

Stronger evidence may be obtained in a system with enhanced production of hydroxyl radicals, since in this case the discriminating capacity of the ration of rate constants, *m*, is higher. The symbols labelled 1–4 in Fig. 5 represent R_{ct}–*m* pairs for reactions carried out in PBW (1–3) and in non-buffered pure water (4). They show that the generation of hydroxyl radicals was considerably enhanced with respect to wastewater. Additionally, in PBW and pure water the hydroxyl radical-to-ozone ratio decreased during the run. The intervals listed in Table 2 and represented in Fig. 5 correspond to the first minute and to the period 6.5 ± 1.5 min respectively. For pure water, only the later is shown as there was no ozone in solution during the first 2 min.

In all cases the experimental value of *m* fell within the theoretical boundaries of $k^{h}_{HO\bullet\,(FFA)}/k^{h}_{HO\bullet\,(ATZ)} = 2.58 \pm 0.55$. This was true both for runs using MnO_x/Al_2O_3 and Al_2O_3, irrespective of the initial concentration of the organic compound, and for runs either in PBW or in pure water. This result shows no evidence that the catalysts contribute to an increase above its homogeneous value in the rate

Table 2
Rate constants for the decomposition of ozone and ratio of the concentration of hydroxyl radical-to-ozone in several matrixes (pH 6.5 in all cases).

	Non-catalytic	Al_2O_3	MnO_x/Al_2O_3
Homogeneous first order kinetic constant for the decomposition of ozone (s^{-1})			
Pure water	$(3.16 \pm 0.35) \times 10^{-3}$	$(5.50 \pm 0.53) \times 10^{-3}$	$(8.82 \pm 0.46) \times 10^{-3}$
PBW	$(2.10 \pm 0.45) \times 10^{-3}$	$(2.48 \pm 0.61) \times 10^{-3}$	$(3.89 \pm 0.28) \times 10^{-3}$
Wastewater[a]	$(4.78 \pm 0.72) \times 10^{-3}$	$(5.14 \pm 0.55) \times 10^{-3}$	$(5.79 \pm 0.67) \times 10^{-3}$
Ratio of hydroxyl radical-to-ozone R^{h}_{ct} or $\bar{R}^{hc}_{ct}$			
Pure water (Av. 2–5 min)	–	–	8.2×10^{-7}
PBW (1st min)	2.0×10^{-7}	4.9×10^{-7}	1.4×10^{-6}
PBW (Av. 5–8 min)	4.7×10^{-8}	9.0×10^{-8}	2.7×10^{-7}
PBW + *t*-BuOH 1.0 mM	–	–	1.6×10^{-9}
Wastewater	9.4×10^{-10}	2.9×10^{-9}	6.2×10^{-9}

[a] Stopped ozone flow after 30 min of semicontinuous ozonation.

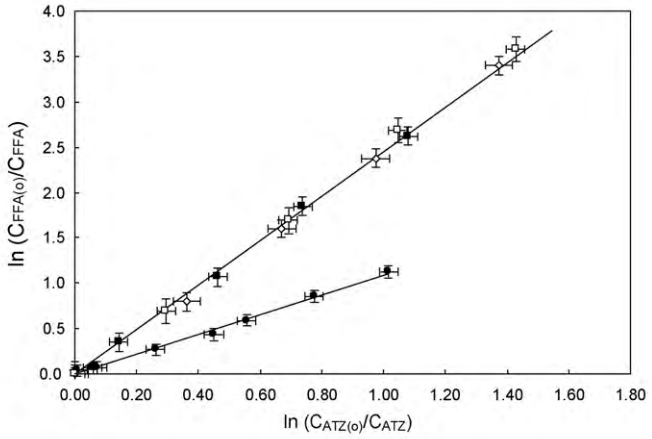

Fig. 6. Logarithmic plot of the concentration of fenofibric acid and atrazine in non-catalytic ozonation (□) and using 1 g L^{-1} MnO_x/Al_2O_3 in PBW (■), in PBW + 1.0 mM *t*-BuOH (●) and in pure non-buffered water (◊). pH was 6.5 in all cases.

constant for the reaction between organics and hydroxyl radicals. The reason may be that the surface interaction with fenofibric acid, if any, was too small to activate the organic molecule through surface bonding. The hydroxyl radical-to-ozone ratio, however, was significantly improved by the use of catalysts. Table 2 shows that the use of Al_2O_3 increased the ratio by up to three times, whereas MnO_x/Al_2O_3 resulted in a seven-fold increase with respect to non-catalytic ozonation using the same substrate concentration. The values were similar in PBW and wastewater, the latter also being reported in Table 2. Fig. 6 shows that in the absence of phosphate, the use of MnO_x/Al_2O_3, whether in PBW or pure water, did not change the slope *m* in Eq. (6). It may be argued that MnO_x/Al_2O_3's failure to affect the rate constant could be attributed to an inhibition of fenofibric acid adsorption due to the phosphate buffer. This behaviour was also observed in pure water making it plain that this is not the case.

The addition of *t*-BuOH 1.0 mM to PBW resulted in apparent kinetic constants that did not change throughout the run. These kinetic constants, k_R, were considerably greater than the direct ozonation constants, k_{O_3}, for fenofibric acid and atrazine, indicating that the amount of *t*-BuOH was insufficient to completely scavenge hydroxyl radicals; but they did not reach the high values of R_{ct} found during the first part of the ozonation runs in the absence of *t*-BuOH. Fig. 7 shows the evolution of the concentration of fenofibric acid and atrazine in the presence of *t*-BuOH 1.0 mM on MnO_x/Al_2O_3 as a function of the integral ozone exposure. The corresponding values of R_{ct} and *m* are also shown in Fig. 5 and again show no deviation from the solid line drawn using homogeneous rate constants.

Fig. 8 plots the average hydroxyl radical-to-ozone ratio as a function of the concentration of fenofibric acid showing that R_{ct} was approximately linear with the concentration of fenofibric acid. This might be a consequence of a promoting effect of fenofibric acid or an ozonation by-product. It is well known that ozone decomposition, as well as the formation of radicals such as superoxide and hydroperoxyl, can be promoted by the presence of certain substances including compounds commonly found as ozonation by-products. In a previous study we identified 2-hydroxyisubutyric acid and some other acidic compounds to be ozonation by-products of clofibric acid, a fibrate with a relatively similar structure [31].

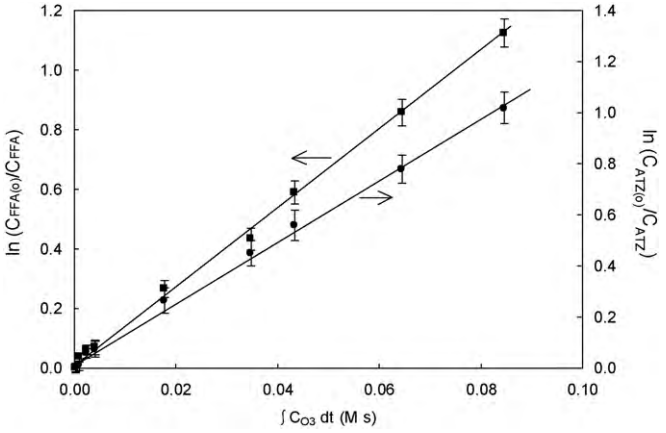

Fig. 7. Concentration of fenofibric acid (■) and atrazine (●) as a function of integral ozone exposure during catalytic ozonation using 1 g L^{-1} MnO_x/Al_2O_3 in PBW + 1.0 mM *t*-BuOH.

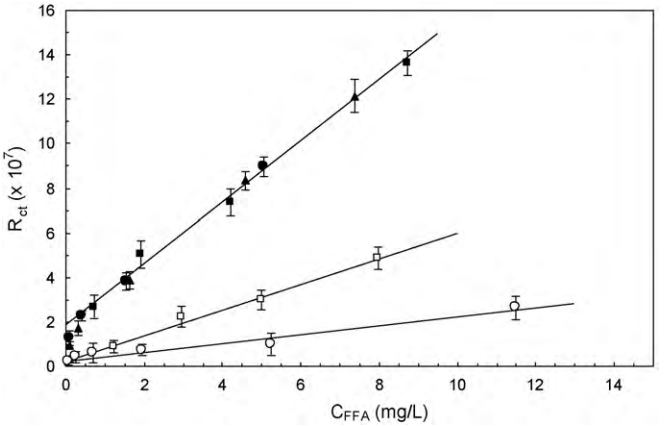

Fig. 8. Average hydroxyl radical-to-ozone ratio as a function of the average concentration of fenofibric acid for non-catalytic ozonation (○) and catalytic reaction using 1 g L^{-1} Al_2O_3 (□) both with 15 mg L^{-1} of initial concentration in PBW. Filled symbols correspond to ozonation with 1 g L^{-1} MnO_x/Al_2O_3 at initial concentration of fenofibric acid of 15 mg L^{-1} (■), 10 mg L^{-1} (▲) and 5 mg L^{-1} (●) in PBW. pH was 6.5 in all cases.

The role of catalytic surface in the heterogeneous decomposition of dissolved ozone was also studied by stopping the gas flow at a given time in order to record the concentration of ozone thereafter until total ozone depletion [18]. In wastewater runs, stopped-flow experiments were performed after 30 min of ozonation to ensure the absence of most reactive compounds. The kinetic constants expressed in pseudo-homogeneous units for a catalyst concentration of 1 g L^{-1} at pH 6.5 are shown in Table 2 for pure water, PBW and wastewater. In all cases the use of catalysts resulted in an increase of the ozone decomposition rate with greater differences in pure water, but following the same trend in PBW and wastewater. The results showed that both catalysts promoted ozone decomposition. Their effect on ozone decomposition was lower than their effect on promoting the generation of hydroxyl radicals. This is not necessarily contradictory, even considering the fact that the generation of hydroxyl radical stems from the decomposition of ozone, as both results refer to quite different situations: batch homogeneous ozone decomposition versus semicontinuous ozonation of organics while continuously bubbling ozone.

This increase in the hydroxyl-to-ozone ratio in catalytic runs supports the common assumption that surface hydroxyl groups formed from the interaction of water with catalyst sites may react with ozone to form a surface complex [12,32]. On a similar basis, several authors have proposed that hydroxide ions linked to negatively charged surfaces initiate ozone decomposition and constitute the true active sites for catalytic ozonation [33,34]. In this study, we have demonstrated that MnO_x/Al_2O_3, negatively charged at pH 6.5, increased the exposure to hydroxyl radicals to a considerably larger extent than activated alumina, whose isoelectric point is 8.2 and was positively charged. This result is consistent with the electrophilic character of the ozone molecule, although the influence of surface charge or the interaction with dissolved ozone is still not clear. The fact that the extent of adsorption did not differ significantly from zero (i.e.: within the uncertainty of the HPLC analytical method) is not fully incompatible with a reaction that takes place between adsorbed species. It is conceivable that a very low concentration of adsorbed fenofibric acid reacts very rapidly with adsorbed hydroxyl radicals but the low rate of adsorption observed in pure water experiments do not support this assumption. Neither does the lack of effect of catalysts on the kinetic constant of hydroxyl-mediated ozonation.

4. Conclusions

Using the competition kinetic method, we determined a rate constant at 20 °C for the non-catalytic ozonation of fenofibric acid of $3.43 \pm 0.20\ M^{-1}\ s^{-1}$. The rate constant for the reaction of fenofibric acid and hydroxyl radicals was $(6.55 \pm 0.33) \times 10^9\ M^{-1}\ s^{-1}$. To our knowledge this is the first time that this rate constant has been reported.

The results of catalytic runs did not show any evidence that the use of Al_2O_3 or MnO_x/Al_2O_3 resulted in an increase in the indirect ozonation rate constant with respect to homogeneous ozonation. This fact suggests the absence of surface interaction with fenofibric acid and may probably indicate that its adsorption did not take place at all. Adsorption data also point in the same direction as neither fenofibric acid nor atrazine adsorb significantly on Al_2O_3 and MnO_x/Al_2O_3 when using PBW and wastewater. Ozonation runs in non-buffered pure water again showed that the tested catalysts had no effect on the indirect ozonation rate constant.

Hydroxyl radical-to-ozone ratio was significantly improved by the use of catalysts. An amount of 1 g L^{-1} of Al_2O_3 increased it up to three times whereas MnO_x/Al_2O_3 resulted in a seven-fold increase with respect to non-catalytic ozonation. This holds true for both PBW and wastewater, with a positive effect of both catalysts even in the presence of salts and radical scavengers. The higher rate of hydroxyl radical generation took place on the most active catalyst for the decomposition of dissolved ozone. This fact is consistent with the assumption that the catalysts promoted the generation of hydroxyl radicals, probably through the formation of surface complexes between ozone and surface hydroxyl groups, even if they do not interact significantly with organics.

Acknowledgements

This work has been financed by Spain's Ministry of Education (CSD2006-00044) and the DGUI de la Comunidad de Madrid, Research Network 0505/AMB-0395.

References

[1] M. Stumpf, T.A. Ternes, R.D. Wilken, S.V. Rodrigues, W. Baumann, Polar drug residues in sewage and natural waters in the state of Rio de Janeiro, Brazil, Sci. Tot. Environ. 225 (1999) 135–141.
[2] T.A. Ternes, J. Stüber, N. Herrmann, D. McDowell, A. Ried, M. Kampmann, B. Teiser, Ozonation: a tool for removal of pharmaceuticals, contrast media and musk fragrances from wastewater? Water Res. 37 (2003) 1976–1982.
[3] J.L. Acero, F.J. Benitez, A.I. Leal, F.J. Real, F. Teva, Membrane filtration technologies applied to municipal secondary effluents for potential reuse, J. Hazard. Mater. 177 (2010) 390–398.
[4] A. Rodríguez, R. Rosal, J.A. Perdigón, M. Mezcua, A. Agüera, M.D. Hernando, P. Letón, A.R. Fernández-Alba, E. García-Calvo, Ozone-based technologies in water and wastewater treatment, in: D. Barceló, M. Petrovic (Eds.), The Handbook of Environmental Chemistry, vol. 5, Part S/2, Emerging Contaminants from Industrial and Municipal Waste, Springer, Berlin, 2008, pp. 127–175.
[5] R. Rosal, A. Rodríguez, J.A. Perdigón-Melón, A. Petre, E. García-Calvo, M.J. Gómez, A. Agüera, A.R. Fernández-Alba, Occurrence of emerging pollutants in urban wastewater and their removal through biological treatment followed by ozonation, Water Res. 44 (2010) 578–588.
[6] R. Rosal, I. Rodea-Palomares, K. Boltes, F. Fernández-Piñas, F. Leganés, S. Gonzalo, A. Petre, Ecotoxicity assessment of lipid regulators in water and biologically treated wastewater using three aquatic organisms, Environ. Sci. Pollut. Res. 17 (2010) 135–144.
[7] I. Muñoz, A. Rodríguez, R. Rosal, A.R. Fernández-Alba, Life Cycle Assessment of urban wastewater reuse with ozonation as tertiary treatment. A focus on toxicity-related impacts, Sci. Tot. Environ. 407 (2009) 1245–1256.
[8] K. Ikehata, N.J. Naghashkar, M.G. El-Din, Degradation of aqueous pharmaceuticals by ozonation and advanced ozonation processes: a review, Ozone Sci. Eng. 28 (2006) 353–414.
[9] B. Legube, Formation of ozonation by-products, in: A. Nikolay (Ed.), The Handbook of Environmental Chemistry, vol. 5, Part G, Haloforms and Related Compounds in Drinking Water, Springer, Berlin, 2003, pp. 95–116.
[10] F.J. Beltrán, F.J. Rivas, R. Montero, Mineralization improvement of phenol aqueous solutions through heterogeneous catalytic ozonation, J. Chem. Technol. Biotechnol. 78 (2003) 1225–1333.
[11] H. Einaga, S. Futamura, Catalytic oxidation of benzene with ozone over alumina-supported manganese oxides, J. Catal. 227 (2004) 304–312.
[12] L. Yang, C. Hu, Y. Nie, J. Qu, Catalytic ozonation of selected pharmaceuticals over mesoporous alumina-supported manganese oxide, Environ. Sci. Technol. 43 (2009) 2525–2529.
[13] B. Kasprzyk-Hordern, M. Ziolek, J. Nawrocki, Catalytic ozonation and methods of enhancing molecular ozone reactions in water treatment, Appl. Catal. B: Environ. 46 (2003) 639–669.
[14] C.M. Jonsson, C.L. Jonsson, D.A. Sverjensky, H.J. Cleaves, R.M. Hazen, Attachment of L-glutamate to rutile (α-TiO_2): a potentiometric, adsorption, and surface complexation study, Langmuir 25 (2009) 12127–12135.
[15] R. Rosal, A. Rodríguez, M.S. Gonzalo, E. García-Calvo, Catalytic ozonation of naproxen and carbamazepine on titanium dioxide, Appl. Catal. B: Environ. 84 (2008) 48–57.
[16] F.J. Beltrán, Ozone Reaction Kinetics for Water and Wastewater Systems, CRC Press LLC, Florida, 2004, pp. 124–125.
[17] M.O. Buffle, J. Schumacher, E. Salhi, M. Jekel, U. von Gunten, Measurement of the initial phase of ozone decomposition in water and wastewater by means of a continuous quench-flow system: application to disinfection and pharmaceutical oxidation, Water Res. 40 (2006) 1884–1894.
[18] R. Rosal, A. Rodríguez, M.S. Gonzalo, E. García-Calvo, Ozonation of clofibric acid catalyzed by titanium dioxide, J. Hazard. Mater. 169 (2009) 411–418.
[19] P.H. Calderbank, M.B. Moo-Young, The continuous phase heat and mass transfer properties of dispersions, Chem. Eng. Sci. 16 (1961) 39–54.
[20] R. Rosal, A. Rodríguez, J.A. Perdigón-Melón, A. Petre, E. García-Calvo, Oxidation of dissolved organic matter in the effluent of a sewage treatment plant by ozone combined with hydrogen peroxide (O_3/H_2O_2), Chem. Eng. J. 149 (2009) 311–318.
[21] W.S. Kijlstra, E.K. Poels, A. Bliek, B.M. Weckhuysen, R.A. Schoonheydt, Characterization of Al_2O_3-supported manganese oxides by electron spin resonance and diffuse reflectance spectroscopy, J. Phys. Chem. B 101 (1997) 309–316.

[22] T. Morimoto, S. Kittaka, Isoelectric point of manganese oxide, Bull. Chem. Soc. Jpn. 47 (1974) 1586–1588.
[23] H. Einaga, M. Harada, S. Futamura, Structural changes in alumina-supported manganese oxides during ozone decomposition, Chem. Phys. Lett. 408 (2005) 377–380.
[24] M.S. Elovitz, U. von Gunten, Hydroxyl radical/ozone ratios during ozonation processes. I. The Rct concept, Ozone Sci. Eng. 21 (1999) 239–260.
[25] U. von Gunten, Ozonation of drinking water: Part I. Oxidation kinetics and product formation, Water Res. 37 (2003) 1443–1467.
[26] F.J. Beltrán, J.F. Garcia-Araya, P.M. Alvarez, F.J. Rivas, Aqueous degradation of atrazine and some of its main by-products with ozone/hydrogen peroxide, J. Chem. Technol. Biotechnol. 71 (1998) 345–355.
[27] J.L. Acero, K. Stemmler, U. von Gunten, Degradation kinetics of atrazine and its degradation products with ozone and OH radicals: a predictive tool for drinking water treatment, Environ. Sci. Technol. 34 (2000) 591–597.
[28] B. Balci, N. Oturan, R. Cherrier, M.A. Oturan, Degradation of atrazine in aqueous medium by electrocatalytically generated hydroxyl radicals. A kinetic and mechanistic study, Water Res. 43 (2009) 1924–1934.
[29] G.U. Buxton, C.L. Greenstock, W.P. Helman, A.B. Ross, Critical review of rate constants for reactions of hydrated electrons, hydrogen atoms and hydroxyl radicals ($HO^{\bullet}/O^{\bullet -}$) in aqueous solution, J. Phys. Chem. Ref. Data 17 (1988) 513–886.
[30] N.K. Vel Leitner, B. Roshani, Kinetic of benzotriazole oxidation by ozone and hydroxyl radical, Water Res. 44 (2010) 2058–2066.
[31] R. Rosal, M.S. Gonzalo, K. Boltes, P. León, J.J. Vaquero, E. García-Calvo, Identification of intermediates and ecotoxicity assessment of the oxidation products generated during the ozonation of clofibric acid, J. Hazard. Mater. 172 (2009) 1061–1068.
[32] H. Jung, H. Choi, Catalytic decomposition of ozone and para-chlorobenzoic acid (pCBA) in the presence of nanosized ZnO, Appl. Catal. B: Environ. 66 (2006) 288–294.
[33] J. Ma, N.J.D. Graham, Degradation of atrazine by manganese-catalysed ozonation: influence of humic substances, Water Res. 33 (1999) 785–793.
[34] F.J. Belltrán, J. Rivas, P. Álvarez, R. Montero, Kinetics of heterogeneous catalytic ozone decomposition in water on an activated carbon, Ozone Sci. Eng. 24 (2002) 227–237.